

Development of Eco-Friendly Soy Protein Fiber: A Comprehensive Critical Review and Prospects

Muneeb Tahir ^{1,*}, Ang Li ¹, Marguerite Moore ¹, Ericka Ford ¹, Thomas Theyson ² and Abdel-Fattah M. Seyam ¹

¹ Wilson College of Textiles, NC State University, 1020 Main Campus Dr., Raleigh, NC 27606, USA; ali10@ncsu.edu (A.L.); mmmoore4@ncsu.edu (M.M.); enford@ncsu.edu (E.F.); aseym@ncsu.edu (A.-F.M.S.)

² TensTech Inc., 1405-B Babbage Lane, Indian Trail, NC 28079, USA; tenstech@earthlink.net

* Correspondence: mtahir2@ncsu.edu

Abstract: In the first half of the twentieth century, scientific communities worldwide endeavored to diminish dependence on expensive and scarce animal fibers like wool and silk. Their efforts focused on developing regenerated protein fibers, including soy, zein, and casein, to provide comparable benefits to natural protein fibers, such as lustrous appearance, warmth, and a soft feel. The popularity and cost-effectiveness of mass-produced petroleum-based synthetic polymer fibers during World War II diminished interest in developing soy protein fiber. Realizing the ecological degradation caused by fossil fuels and their derived products, a renewed drive exists to explore bio-based waste materials like soy protein. As a fast-growing crop, soy provides abundant byproducts with opportunities for waste valorization. The soybean oil extraction process produces soy protein as a byproduct, which is a highly tunable biopolymer. Various functional groups within the soy protein structure enable it to acquire different valuable properties. This review critically examines scholarly publications addressing soy protein fiber developmental history, soy protein microstructure modification methods, and soy protein fiber spinning technologies. Additionally, we provide our scientific-based views relevant to overcoming the limitations of previous work and share prospects to make soy protein byproducts viable textile fibers.

Keywords: soy protein; waste valorization; sustainable fiber; tunable biopolymer; soy protein fiber spinning; soy protein fiber commercial viability



Citation: Tahir, M.; Li, A.; Moore, M.; Ford, E.; Theyson, T.; Seyam, A.-F.M. Development of Eco-Friendly Soy Protein Fiber: A Comprehensive Critical Review and Prospects. *Fibers* **2024**, *12*, 31. <https://doi.org/10.3390/fib12040031>

Academic Editor: Marija Gizdavic-Nikolaidis

Received: 13 February 2024

Revised: 23 March 2024

Accepted: 26 March 2024

Published: 30 March 2024



Copyright: © 2024 by the authors. Licensee MDPI, Basel, Switzerland. This article is an open access article distributed under the terms and conditions of the Creative Commons Attribution (CC BY) license (<https://creativecommons.org/licenses/by/4.0/>).

1. Introduction

Plastic pollution is a poignant symbol of our environmental reality. Over 8,300 million metric tons of plastics were produced by 2017, with half produced between 2002 and 2015 [1]. In addition to plastic's long degradation periods, the shedding of micro- and nanoplastics poses a significant ecological and health hazard. Microplastics are finding their way into our terrestrial [2] and aquatic [3] food sources, air [4], and even human wombs [5]. In addition to micro/nanoplastic pollution, effective management of macroplastic waste is a significant challenge, with 22% not being collected, 19% incinerated, and 50% dumped in landfills [6]. Dwindling landfill numbers [7] and government-imposed taxes on landfill operations [8] complicate waste disposal and increase business costs.

Synthetic textile fibers accounted for 12% of total plastic production until 2017 [1], contributing to around 35% of ocean microplastics [9]. As 63% of textile fibers are synthetic [10], adopting eco-friendly and sustainable textiles is essential to combat environmental degradation. In 2022, the US produced approximately 122.469 million metric tons of soybeans, with global production projected to reach 410.6 million metric tons for 2022–2023 [11]. The rise of soy-based biofuels and renewable diesel as alternatives to petroleum has spurred the establishment of numerous crushing plants in US states [12,13]. This transition creates a surplus of soy protein, presenting an economically viable opportunity for valorization and gaining market share by replacing synthetic materials in high-volume manufacturing sectors like textiles.

Interest in soy protein textile fibers dates back to the 1930s [14]. Various methods, including electrospinning, solution blowing, wet spinning, and melt spinning, have been utilized to produce micron/submicron-scale soy protein fibers [15–17]. These fibers have found applications in a wide range of fields, such as controllable lithium (Li) deposition in Li metal batteries [18], sorbents for treating petroleum-contaminated water [19], fabrication of electromagnetic interference shielding [20], drug delivery systems, scaffolds for human tissue growth [21], and alternatives to cotton fibers in knitted cotton fabrics [22,23], to name a few.

The global market for textile fibers was estimated at 116 M tons in 2022 and is projected to reach 147 M tons in 2030 [24]. This surge in textile fiber demand has been met mainly by the booming production of petroleum-based synthetic fibers, which are synthesized from hazardous chemicals and do not decompose naturally [25]. Synthetic fibers dominate the market, making up approximately 65% of the global fiber production in 2022, with cotton's share accounting for merely 22%. Other plant fibers, manmade cellulosic fibers, and animal fibers had significantly smaller market shares of approximately 5.2%, 6.3%, and 1.6%, respectively [24]. However, due to erratic oil prices and supply, the cost and availability of synthetic fibers have become a concern. The price of the most widely used polyester fibers has more than doubled in the last decade and is expected to continue to increase. On the other hand, the cultivation of textile natural fibers, such as cotton, is declining as farmers increasingly shift resources to grow crops with higher economic returns [26]. Therefore, considering the substantial market size of textile fibers, finding abundant, economical, and sustainable alternatives becomes critical.

The need to develop eco-friendly fibers to replace fossil-fuel-based fibers, the market size of textiles, and the opportunities to convert the abundant soy byproducts' waste to viable textile fibers prompted our team to undertake this comprehensive critical review. The review covers the means of modifying soy protein microstructure, chronology of soy protein fiber development, characterization of soy protein fiber spinning techniques, and critical analysis of the existing research literature in these areas. In conclusion, we also address the challenges and opportunities for developing soy protein fiber.

2. Development of Soy Protein Fibers in History

2.1. *The Interwar Period: 1937–1939 Second World War*

Before World War II, global powers recognized their dependence on wool-based military clothing and sought synthetic protein fibers as alternatives [27]. Inspired by the development of casein and fish protein fibers in Italy and Germany, Japan pioneered regenerated soy protein fiber (RSPF), filing a US patent in 1937 [14,28] and producing 1 million lbs. of RSPF by 1939 [29]. However, the reasons for RSPF's limited utilization during World War II in Japan are poorly documented in the English academic literature.

Meanwhile, in the US, Robert A. Bouyer, leading a Ford Motor Company (FMC) research laboratory, presented the first American RSPF to the Fourth Annual Conference of the Farm Chemurgic Council in 1938. This RSPF's intended use was making automotive sidewall upholstery [30,31]. FMC's founder, Henry Ford, championed soybean as a panacea to the economic ailments of the Great Depression, promoting soybeans as a simultaneous source of food, clothing, and car-making material [30]. Ford's efforts included wearing garments made from RSPF, such as a necktie and a suit containing 50% and 25% RSPF, respectively, to promote RSPF as a textile and apparel material [30].

2.2. *Soy Protein Fiber during the Second World War: 1939–1945*

By 1940, FMC's pilot plant was producing 4400 lbs. of RSPF daily, with Bouyer claiming it was 80% as strong as wool fiber and had higher wet and dry elongation. Furthermore, in 1940, the Drackett Company collaborated with FMC to supply spinnable soy protein for upholstery fabrics [32]. Soy protein's economic potential was identified in a 1942 wartime US government report, which maintained that it could be produced at half the cost of wool fiber [33]. However, its applicability in peacetime remains uncertain.

In 1943, Henry Ford halted FMC's RSPF work, and Drackett Company acquired FMC's fiber spinning setup. Robert A. Bouyer joined Drackett as the director of scientific research. However, puzzlingly, the commercially produced RSPF at the Drackett Company had inferior mechanical properties compared to the fiber produced at FMC under Bouyer's supervision. A comparable grade of wool fiber exhibited dry and wet strengths that were 45% and 76% higher than the Drackett RSPF [30]. Despite this, Drackett's "Soybean" Azlon was found to be used mainly in felted hats, with plans to enter other textile markets with blended soy fiber [32].

2.3. Post-World War II Period: 1946–1961

Interest in RSPF emerged during World War II to address potential wool supply chain challenges. However, low wet strength, processing complexities, competition from cost-effective petroleum-based synthetic fibers, adverse consumer perceptions linked to wartime scarcity necessitating the development of these fibers, resource redirection from fiber-making endeavors toward positioning soy protein as a human nutrition source, and declining wool prices in the aftermath of the war hindered RSPF's commercial viability post-war [34–36], and the commercialization of patented production technologies failed. The Drackett Company's decision to scale back on the commercial production of its soybean Azlon and focus solely on basic experimental endeavors in this area reflects these realities. Incidentally, this is when Bouyer left the Drackett Company to work on meat-substituting edible soy protein fibers [32].

Despite elusive commercialization, research into the wet spinning of RSPF continued, leading to various patent filings to improve its mechanical performance and characteristics [37–45].

2.4. Contemporary Period: 1995 to Date

Since the late twentieth century, there has been a renewed interest in soy protein fibers due to growing environmental consciousness. Around the second half of the twentieth century, the first alarm bells rang, noting the dangers of large-scale plastic consumption [46]. Subsequently, research into sustainable textile fibers like soy protein fibers gained momentum in response to the mounting evidence of environmental threats posed by plastics. China, a significant cashmere fiber supplier, emerged as a leader in exploring the potential of soy protein fibers as a substitute for "sheep" cashmere, driven by the imperative to combat desertification resulting from the extensive grazing of cashmere sheep and ecological concerns linked to the consumption of synthetic textiles [47]. Changes in the global trade landscape may enhance the potential for improved cost-effectiveness of Chinese-developed soybean fiber, which is more affordable than cashmere and silk fibers it aims to replicate [48]. Typically, producing durable textiles necessitates fiber tenacity values exceeding 2.5 g per denier (g/denier) or 2.207 centinewtons per decitex (cN/dtex). However, textiles made from lower-strength fibers, such as wool, can still be viable despite tenacity values below 2.5 g/denier, attributed to their notable elasticity [49]. Wool fibers exhibit resilience, characterized by the elongation at break of 35% in dry and 45% in wet conditions (Grishanov 2011). Consequently, in the context of textile manufacturing, Table 1 illustrates the comparatively inferior mechanical properties of soy protein fibers documented in the literature from the late twentieth and early twenty-first century researchers.

Table 1. Effect of soy protein feedstock preconditioning, fiber processing conditions, and post-treatments on spun fiber mechanical performance.

Fiber Type and Diameter or Linear Density	Spinning Type and Extrusion Temp.	Raw Material and Fiber Conditioning			Tensile Modulus (MPa)	Tensile Strength (MPa)	Tenacity (cN/dtex)	Elongation at Break (%)	Ref.
		Denaturing Mode and Conditions	Coagulation Bath Composition and Temperature	Post-Spinning Treatment					
10 wt.% soy protein/alginate Diameter < 80 μm	Wet spinning at 25 °C	10 wt.% sodium hydroxide aqueous solution at room temp.	10 wt.% calcium chloride + 1 wt.% HCL + 0 wt.% ethanol	20% drawing	-	-	1.41 (dry), 0.34 (wet)	21.7 (dry) 46.4 (wet)	[50]
10 wt.% soy protein/PVA Neither diameter nor linear density provided	Wet spinning at 70 °C	Aqueous solvent of urea + sodium sulfite + 85 °C heating	Sodium sulfate and ammonium sulfate in water with 1 M sulfuric acid	Glutaric dialdehyde crosslinking followed by heating at 190 °C at 20 MPa stress	5300 ± 300	260 ± 11	-	11 ± 0.6	[51]
Regenerated 100% soy protein, Diameter of 50–150 μm	Wet spinning	8 M urea solution with 1% (w/w) sodium sulfite, soy protein solution aged 96 h at room temperature	10% (w/w) sodium sulfite and 10% (w/w) acetic acid fibers remain in the bath for 30 min	-	6500 ± 1700	145 ± 10	-	8 ± 2	[26]
Regenerated 100% soy protein fiber, Diameter < 368 μm	Wet spinning	Sodium hydroxide aqueous solution at pH 12.1	4% hydrochloric acid solution containing 3.3% sodium chloride, 3.3% zinc chloride, and 3.3% calcium chloride	25% glutaraldehyde and drawing to 170% as-spun length	-	-	0.638 and 0.73 at 0.65 and 1 water activity levels	3.1 and 59.7 at 0.65 and 1 water activity levels	[16]
45 wt.% soy protein/15 wt.% glycerol/40 wt.% water, Diameter < 368 μm	Melt spinning at 96 °C and 20 rpm	96 °C temp + 20 rpm in a twin-screw extruder	-	glutaraldehyde + acetic anhydride and drawing to 150% as-spun length	-	-	0.53 and 0.24 at 0.65 and 1 water activity levels	9.2 and 39.3 at 0.65 and 1 water activity levels	[16]
Regenerated 100% soy protein, Diameter 50 μm	Wet spinning	8 M urea solution with 1.1% (w/w) sodium sulfite, heated for 2 h at 80 °C, solution aged for 2 days	Citric acid, sodium sulfate, zinc sulfate, and water (1:1:0.1:8 w/w), bath's pH 2.2	-	523 g/tex (4801 MPa)	-	0.9	5–9	[52]
10 wt.% SPI-g-PAN, Diameter < 11 μm	Wet spinning at 70 °C	DMSO + BMIMCl at 75 °C	Water and ethanol (1:1) constant temperature at 4 °C	-	1478.4 ± 185	512.6 ± 76.9	-	11.87 ± 1.1	[53]

Table 1. Cont.

Fiber Type and Diameter or Linear Density	Spinning Type and Extrusion Temp.	Raw Material and Fiber Conditioning			Tensile Modulus (MPa)	Tensile Strength (MPa)	Tenacity (cN/dtex)	Elongation at Break (%)	Ref.
		Denaturing Mode and Conditions	Coagulation Bath Composition and Temperature	Post-Spinning Treatment					
45 wt.% soy protein/ 15 wt.% glycerol/ 40 wt.% water, Diameter < 368 μ m	Melt spinning at 96 °C and 20 rpm	96 °C temp + 20 rpm in a twin-screw extruder	-	89 wt.% water/9.5 wt.% ethanol/ 1.5 wt.% 1,4-benzoquinone	2552.04 \pm 238.68 g/tex (11 rh) 2570.4 \pm 330.48 g/tex (65 rh) 293.76 \pm 55.08 g/tex (100 rh)	-	0.354 at 11% rh 0.337 at 65% rh 0.053 at 100 rh	-	[54]
15 wt.% soy flour/ PP + monoglyceride compatibilizer	Melt spinning at 190 °C	190 °C temp + 100 rpm in twin screw for 2 min	-	100 draw-down ratio	914 \pm 164	74 \pm 7	-	268 \pm 57	[55]
23 wt.% soy flour/ 7 wt.% monoglyc- eride/70 wt.% LLDPE, Diameter 45 \pm 11 μ m	Melt spinning at 140 °C	140 °C temp + 100 rpm twin screw extruder	-	-	615 \pm 38	57.0 \pm 8.0	-	280 \pm 29	[56]

3. Soy Protein Structure and Extraction

Soy protein possesses a hierarchical structure characterized by multiple organizational levels, extensively discussed in the scientific literature [57–60]. Comprehending the hierarchical organization of soy protein is imperative to elucidate its functional properties and potential application as a spinnable textile fiber. Modifying the native soy protein structure is essential for transforming this biopolymer into spinnable fiber. The following section critically evaluates various methods for modifying the soy protein structure. Additionally, a comprehensive understanding of extraction processes for obtaining protein-rich, spinnable soybean products, such as defatted soy flour and soy protein isolate (SPI), is available in the existing literature [61–63]. Low-value protein-rich soy flour and SPI are byproducts of the soybean oil extraction.

4. Soy protein Structural Modification

An abundance of chemical moieties like amino, carboxyl, hydroxyl, sulfhydryl, and phosphate make soy protein amenable to structural modification. These modifications tailor the protein's properties to meet specific application requirements and facilitate soy protein fiber spinning. The following sections detail these modification techniques, while Table 2 summarizes the utility and drawbacks of various soy protein structural modification techniques.

Table 2. Advantages and disadvantages of various soy protein structural modification techniques.

Structural Modification Techniques	Advantages	Disadvantages
Denaturation	Increased compatibility with hydrophobic thermoplastic matrices due to exposure of hydrophobic groups buried deep within the coiled soy protein structure.	Soy protein aggregation post-denaturation due to new protein–protein interactions. These aggregates can plug the spinnerets or the screens/filters during the fiber formation. Exposure of soy protein's hydrophobic groups can aid the processibility in melt spinning; however, in the case of wet spinning, the solubility of the protein in aqueous solvents can decline.
Acetylation	Acetylation makes soy protein less polar and, hence, more hydrophobic. Induced hydrophobic character can increase soy protein's compatibility with nonpolar matrices, amplifying its processibility in melt spinning.	The increased hydrophobic character of acetylated soy protein can compromise their solubility in aqueous solvents during wet spinning.
Esterification	Subdued soy protein brittleness post-esterification.	The increased isoelectric point of esterified soy protein necessitates using environmentally harmful, highly acidic, or basic conditions for its solubility, which is vital for preparing wet-spinnable dopes.
Graft polymerization	The highly tunable nature of soy protein due to an abundance of chemical moieties enables its grafting with select monomers. Strong linkages can then be established between the polymeric matrices or solvents and grafted soy proteins, enhancing the mechanical properties of the resultant spun fibers.	Limited grafting monomer choices.

4.1. Denaturation

Denaturation, or destructureation, involves a protein losing its secondary, tertiary, and quaternary structures while preserving its primary structure. In its native form, soy protein adopts a three-dimensional globular conformation. Unfolding soy protein's native globular conformation allows the denatured protein subunits to entangle with each other and enable the spinning of soy protein fibers [52].

Various conditions, such as heat, highly acidic or alkaline environments, reducing agents, organic solvents, and inorganic salts, can denature proteins to varying degrees depending upon the denaturation mode employed. These denaturing agents disrupt hydrogen, ionic, hydrophobic, and disulfide bonds in the native protein structure, unfolding the protein chains. Thermal denaturation involves increasing the vibrational energy of protein molecules to break hydrogen and hydrophobic bonds. Highly acidic or alkaline conditions cause the ions in acids and bases to interchange with the ions of the salts formed by ionic interactions in the protein, breaking these bonds. Reducing agents break the strongest covalent disulfide bonds in the tertiary soy protein structure, and heat-induced breakage of protein disulfide bonds in a basic environment can also occur [64]. Reducing agents can significantly modify soy protein solutions' rheological behavior, enhancing their processability [65]. Their use can improve the spinnability of soy protein fibers on a commercial scale. Organic solvents can sever the hydrophobic interactions between nonpolar side groups of amino acids to transform native protein structures [66]. Inorganic salts destabilize the native protein structure by stripping away water molecules from the protein surface, causing its denaturation [67].

Protein denaturation can cause new protein–protein interactions and increased soy protein system viscosity [62]. Denaturation can also expose buried hydrophobic groups in protein structure, causing undesired protein aggregation [68,69]. However, this exposure to nonpolar hydrophobic groups improves compatibility with nonpolar polymeric matrices [70]. Denaturing agents like urea, sodium dodecyl sulfate, and sodium hydrogen sulfite unfold soy protein chains and enhance the surface hydrophobic index of soy protein [71].

Deviation from the isoelectric points of glycinin (pH 4) and conglycinin (pH 6) accelerates protein denaturation, increasing viscosity in soy protein due to the need for more energy input to align molecules in the flow direction [62]. However, soy protein viscosity drops at pH 9 and 90 °C compared to unheated protein exposed to pH 9. This drop is attributed to the rearrangement of protein subunits during denaturation, resulting in a more soluble soy protein form [72]. Alternatively, protein polypeptide backbone breakage at high pH, i.e., degradation, is also linked to the heat-induced decline in protein viscosity [73].

Thermal treatments render soy protein insoluble through denaturation [74]. However, combining heat treatment with highly acidic or alkaline pH transforms the protein structure, allowing the solvent to access reactive sites in the secondary protein structure, thereby increasing the protein's solubility [72].

4.2. Acetylation

In protein structures, polar groups like hydroxyl, phenols, and lysine's ϵ -amino can undergo acetylation by adding acetyl groups to specific amino acids within the protein, typically achieved through a reaction with acetic anhydride [62,75]. Neutral acetyl groups reduce positive charges in the protein structure under acidic conditions, lowering the isoelectric point of soy protein and increasing its solubility in the pH range of 4.5–7. Acetylation also diminishes the water-binding capacity of soy protein [76]. Lysine acetylation in soy protein's isolated glycinin (11s) fraction increases protein surface hydrophobicity by two-fold beyond 95% acetylation [77]. Soy protein acetylation is accompanied by the decomposition of higher-molecular-weight 11s soy protein sedimentation fraction into lower-molecular-weight 2s and 7s fractions [76]. Complete denaturation of glycinin occurs above 65% lysine acetylation, while below this threshold, soy glycinin's physicochemical properties remain unchanged [77].

Acetylated soy proteins enhance the interaction with nonpolar thermoplastic elastomers (TPE) by inducing hydrophobic character in hydrophilic soy proteins. A 10 wt.% acetylated defatted soy flour/TPE composite exhibits tensile strength comparable to neat TPE's 1.32 ± 0.184 MPa and slightly higher elongation at 71.8 ± 17.3 mm compared to neat TPE, highlighting improved soy protein and hydrophobic matrix compatibility post-acetylation [78]. Acetylated soy protein films molded at 115.6 °C show a higher tensile

strength of 2.21 MPa compared to 1.88 MPa at 93.3 °C despite some molecular weight loss at the higher temperature [79].

4.3. Esterification

Esterification of polar carboxyl groups in soy protein leads to the formation of less polar esters, which reduces the ionic interactions partially responsible for protein brittleness. Consequently, esterification enhances soy protein plastic tensile strength and elongation [62]. Esterification can also alter the protein's isoelectric point alongside acetylation. Esterification of soy proteins can elevate their isoelectric point to 8 from 4.5 [80]. Ethanol-esterified soy proteins acquire positive charges in weakly acidic environments, which helps curtail the growth of bacteria with negatively charged cell membranes [81].

4.4. Soy Protein Graft Copolymerization

Soy protein's abundance of functional groups makes it an attractive candidate for grafting various monomeric and polymeric systems to configure its physicochemical and mechanical properties for specific applications.

Graft yield decreases after the optimum reaction time due to initiating species depletion. At temperatures beyond 90 °C, graft yield drops due to the neutralization of initiating species. Increasing the concentration of SPI enhances the graft yield, but beyond an optimum level, the SPI macroradical combination and disproportionation surpass their combination with polylactide molecules [82].

Polymer grafting disrupts native soy protein structure, increasing solubility and enabling fiber spinning [53]. Sodium metabisulphite cleaves disulfide bonds during protein denaturation, promoting the emergence of suitable sites for radical formation and acrylate monomer grafting. SPI-grafted acrylate films become stiffer with an increasing soy protein fraction, making them ideal for wood coating due to improved wear and scratch resistance [83]. Ionic solvents facilitate soy protein denaturation for graft copolymerization, lowering thermal stability in highly denatured SPI. However, due to crosslinking between glycidyl methacrylate (GMA) and SPI, GMA-grafted SPI exhibits enhanced thermal stability. GMA and acrylate polymers can confer their hydrophobic character to grafted SPI surfaces [84]. Acrylic acid-grafted SPI films show a remarkable 318% increase in tensile strength and a 60% increase in elongation compared to water-soluble polyvinyl alcohol (PVA) films, offering superior adhesion and water solubility for eco-friendly warp yarn sizing applications [85]. Grafted poly(methyl acrylate) soy protein fibers lose their reactive, polar sites during grafting. As a result, they become less receptive to interactions with water molecules [86].

5. Soy Protein Fiber Spinning Techniques

Developmental efforts and scientific investigations into soy protein fiber can be classified based on fiber size. Fiber size, in turn, is a function of the fiber production technique. Therefore, manufacturing methodology dictates the characteristics and potential areas of application of soy protein fiber.

5.1. Techniques for Spinning Submicron-Scale Soy Protein Fibers

5.1.1. Electrospinning

Electrospinning involves extruding an electroactive polymer solution/melt through a fine nozzle at high voltage. Repulsion between like charges on the polymer surface overcomes surface tension to create a charged jet. This jet is drawn and guided to a grounded collector, forming fibers with diameters ranging from micron to submicron scales [87,88]. Electrospun fibers are crucial for applications in tissue engineering, drug release, wound healing, antimicrobial packaging, and filtration due to their high surface area and precise fabrication of submicron-scale fibers. However, scaling up production through electrospinning to meet the demands of high-volume application areas such as

apparel and home textiles is not feasible. So, this technology remains limited to small-scale manufacturing.

Degradation of synthetic polymer-based tissue scaffolds can elicit localized pH decline, cell damage, and immune responses [89]. Using non-toxic soy protein is advantageous, as it exhibits anti-inflammatory properties [90,91]. Cryptic degradation products of functionally active soy proteins promote dermal tissue regeneration [91–94]. Electrospun soy protein scaffolds also reduce inflammatory and immune responses in vivo compared to animal-based scaffolds [91]. Moreover, these scaffolds exhibit superior cellular adhesion compared to solution-casting film structures [95]. The hydrophilic nature of soy protein scaffolds enhances cellular attachment. This hydrophilicity renders soy protein susceptible to dissolution and degradation in aqueous environments [96]. Photo-assisted crosslinking with methacrylic anhydride (MA) can enhance the stability of electrospun soy protein isolate methacrylic anhydride (SPIMA) scaffolds in water compared to non-crosslinked SPI scaffolds. Photo-induced crosslinking of electrospun SPIMA fibers flattens and increases their diameter while reducing the scaffold porosity [97,98]. Crosslinking of proteins generally leads to an increase in protein aggregate sizes, accompanied by both increments and declines in molecular weight and solubility, respectively. Moreover, the crosslinking degree correlates with a proportional elevation of the protein denaturation temperature [62].

Traditionally, researchers have used toxic crosslinkers like aldehydic compounds to improve the stability of electrospun soy protein structures on aqueous exposure. However, due to ecological concerns, researchers are exploring green alternatives like oxidized sucrose (OS), which offers higher crosslinking potential through aldehyde group interactions with protein amino groups. OS acts as a plasticizer, reducing viscosity and promoting molecular mobility in the SPI-PEO-acetic acid electrospinning solution [99]. Water-stable electrospun SPI scaffolds have also been developed for dermal tissue engineering without additional crosslinking agents [91,100].

The joint SPI-PEO system enables electrospinning of fibers, which is not possible with SPI or PEO alone. Denaturation of SPI under highly alkaline conditions (pH 13) and elevated temperature (60 °C) allows PEO's hydrophilic ether oxygen and hydrophobic ethylene segments to form linkages with protein amino acids. Increased denatured SPI concentration enhances solution processability through more unfolded chains, while higher PEO concentration with constant SPI content enhances chain entanglement. This combined effect of chain unfolding and increased chain entanglements leads to elevated system viscosity, preventing the formation of bead-forming droplets in the spinning jet during electrospinning [101]. Increased spinning solution viscosity elevates the fiber diameter by impeding the stretching of the liquid jet [101–104]. A higher soy protein content in its native globular form in a polymeric system leads to electrospun fibers with larger diameters [105] and irregular morphology [106]. A larger average fiber diameter is associated with reduced porosity in electrospun scaffolds [105,107]. However, in the electrospinning of silk fibroin (SF)-SPI-formic acid system, the highest SPI/SF ratio (75/25 wt./wt.) showed the lowest average fiber diameter without explanation [107].

Small-diameter electrospun fibers promote enhanced cellular adhesion and proliferation due to their larger surface area and the high porosity of the electrospun structures they constitute [108]. Highly porous structures facilitate efficient moisture vapor transfer in wound management [109]. Electrospun mats with larger fiber surface area and porosity also improve the release of drug and germicidal agents incorporated within these systems [110]. Drug incorporation in the solution reduces electrospun soy protein fiber diameter by reducing solution viscosity as a plasticizing agent [105,109]. Furthermore, the addition of charged nanostructures to soy protein electrospinning solutions enhances solution electrical conductivity, leading to the formation of smaller-diameter nanofibers. Compatible nanomaterials can also form robust chemical linkages in the spinning solution, increasing solution viscosity and yielding larger average electrospun fiber diameter [102]. Micro/nanoscale fillers enhance the mechanical properties of electrospun soy protein fibers like Young's moduli [111]. However, balancing scaffold rigidity and flexibility is essential

to avoid inflammatory responses and to mimic biomaterial characteristics [112,113]. Soy protein scaffolds exhibit a typical J-shaped stress–strain curve, which is advantageous for *in vitro* implantation in human applications [96].

Superior cellular adhesion and proliferation in electrospun scaffolds are associated with uniform fiber morphology without bead defects [97,108]. A decrease in the electrical conductivity of the electrospinning solution is correlated with improved fiber processibility and enhanced uniformity in fiber morphology [114]. High relative humidity (RH) during electrospinning can lead to bead formation and disrupt homogeneous filler dispersion [98,111]. Bead formation typically occurs when the spinning solution viscosity decreases, and the solution's surface tension favors the assumption of spherical geometry when the solution's surface tension prefers assuming spherical geometry [115]. Adjusting the ambient RH enables the controlled release of allyl isothiocyanate, an antibacterial agent loaded into soy protein-poly(lactic acid) and soy protein-PEO electrospun fibrous mats, thereby offering potential applications in food packaging [116].

5.1.2. Solution-Blown Spinning

Solution-blown spinning offers a ten times faster deposition rate of spun fibers on a substrate than electrospinning, making it potentially suitable for industrial-scale production [117,118]. This technique utilizes a solvent-dissolved polymer pumped through an inner nozzle while a pressurized air jet flows around it, aerodynamically blowing and stretching fibers from the polymer solution. The air also plays a role in solvent evaporation. The resulting fibers, ranging from 100 nm to over 1 μm in diameter, are deposited on a collector [117]. However, like electrospinning, solution-blown spinning of soy protein alone is not feasible and requires a solubilized long-chain polymeric system for fiber production.

Solution-blown spun (SBS) soy protein/nylon-6 nanomembranes efficiently adsorb lead ions at the soy protein's isoelectric point (pH 4.5). Hydroxyl, carboxyl, amine, sulfhydryl, and phenolic groups in soy protein biopolymer-based nanomembranes make them highly suitable for lead ion removal due to the chemical affinity between these groups and lead ions [118]. Bactericidal silver-nanoparticle-infused SBS soy protein nanofiber mats are also suitable for filtration and wound dressing applications, offering an open and porous structure with a substantial contact area for effective attachment of bactericidal nanoparticles, surpassing traditional two-dimensional film-based filter structures [119].

Increasing soy protein content in a spinning solution reduces the resultant fiber web stiffness [17]. Another consequence of increasing soy protein concentration in spinning dope is the production of nanofibers with low diameters due to decreased apparent viscosity and surface tension. These fibers can be highly valuable for various applications due to their large surface area [120]. Using a larger die diameter can cause incomplete evaporation of the aqueous element of the solvent. Insufficient aqueous evaporation at $<180^\circ\text{F}$ air jet temperature leads to fiber roping and fusion, causing diameter variability in the produced fibers. Air jet temperatures $>180^\circ\text{F}$ can clog exit nozzles, and <20 psi air pressure merges adjacent droplets at exit nozzles [17].

Changes in the mechanical characteristics of SBS soy protein/nylon-6 nanofiber mats crosslinked via different modes and agents have been comprehensively studied [121]. Ionic crosslinkers, including sodium borohydride and zinc sulfate, enhance Young's modulus of soy protein nanofiber mats more effectively than crosslinking aldehydes like formaldehyde and glyoxal. However, the opposite trend is observed regarding strain at the break of SBS nanofiber mats. This indicates that ionic crosslinks between protein chains are more robust than crosslinks formed by covalent crosslinkers. Glyoxal-crosslinked nanofiber mats are stiffer than formaldehyde-crosslinked mats among aldehydes because they have more crosslinking aldehyde groups. Overall, all crosslinked specimens demonstrate improved Young's modulus compared to non-crosslinked ones. Upon exposure to thermal energy, the crosslinks break, protein mobility is restored, and Young's modulus values decrease. Exposure to water coupled with 80°C enhances strain at rupture due to the plasticizing influence of water [121].

The core–shell fiber structure, with a soy protein core and a nylon-6 sheath, allows for higher soy protein loading in solution-blown spun fibers compared to monolithic soy protein/nylon-6 fibers. However, nylon-6 still has to be included in the core to ensure the spinnability of the solution through the core nozzle [122]. Thanks to the nylon-6 sheath, the core–shell structure exhibits superior resistance to soy protein dissolution in water compared to crosslinked and non-crosslinked SBS soy protein/nylon-6 nanofiber mats [121]. The hydrophilicity of nylon-6 itself in the SBS soy protein/nylon-6 core–sheath nanofiber web has yet to be addressed due to its amide bonds leading to water absorption and can affect weight loss measurements. Modifying the annular nozzle design by positioning the core spinning nozzle toward the interior prevents nozzle clogging caused by premature air-induced solidification of the material exiting the core nozzle [123].

5.2. Micron-Scale Spinning Techniques

5.2.1. Melt Spinning

Melt spinning is a cost-effective and prevalent fiber production technique that avoids using expensive and toxic solvents. It involves melting thermoplastic polymer pellets or powders in an extruder and feeding the molten polymer to a metering pump that controls the spinneret's melt feed rate. The spinneret extrudes the molten polymer through multiple holes to form multifilament or multiple fibers that are then quenched, drawn, and taken up. Monofilament or a single fiber can also be melt-spun using a single extrusion orifice.

The melt spinning of soy protein textile fibers has received limited attention in the scientific literature compared to other spinning techniques, indicating processing challenges and performance issues in melt-spun fibers.

In their seminal 1995 study, Huang et al. investigated soy protein extrusion/melt spinnability [16]. Melt spinning of soy protein alone has yet to be achieved due to its very high viscosity. Adding an optimum quantity of water to soy protein serves as a plasticizer to bring the mixing torque within the extruder's design limitations. At higher water activity levels, water–protein interactions dominate over protein–protein interactions, reducing fiber tenacity but increasing molecular mobility. Introducing glycerol plasticizer to the soy protein/water melt spun system in the melt spinning stage improves the fiber flexibility and, in some cases, tenacity [16]. Therefore, Huang et al. chose a 45% soy protein/40% water/15% glycerol formulation for spinning multifilament via 386 μm holes. The selection of smaller-hole-sized spinnerets resulted in clogging [16]. The initially flexible spun soy protein fibers became brittle with moisture evaporation. Aging the fibers in moist conditions restored flexibility [16], though long-term moisture loss could diminish this effect. Pre-spinning chemical modifications do not improve fiber tensile performance, but post-treatment with acetic anhydride (acetylation) and acetaldehydes boosts tenacity and elongation in soy protein fibers by replacing polar amines with less polar moieties at different water activity levels while also reducing moisture absorption in the treated fibers. Crosslinking agents can increase fiber tenacity but lower elongation at break, with glutaraldehyde being a more effective crosslinker for soy protein fibers than glyoxal. Drawing acetic anhydride-treated fiber achieves the highest tenacity among soy protein fibers [16], although it still falls significantly below the tenacity of cotton or wool fibers. Huang et al.'s seminal work was further developed by introducing less polar zein protein to soy protein, assuming that less moisture intake of the resultant melt-spun fiber would result in an improved, more tenacious fiber [54]. The optimal soy protein/zein ratio was 80%/20% of the total protein content in the 45% protein/40% water/15% glycerol formulation. Increasing the zein content beyond this ratio resulted in progressively more brittle and less tenacious fiber [54]. However, the tenacity values of the post-treated and drawn soy protein/zein blended fibers using 1,4-benzoquinone, dimethylformamide, and dimethyl sulfoxide remained lower compared to Huang et al.'s acetic anhydride and glutaraldehyde-treated and drawn soy protein fibers [16,54].

Compounding soy flour with petroleum-based thermoplastic polymers like polyethylene (PE), polypropylene (PP), and poly(lactic acid) (PLA) is another strategy to melt spin

soy-based fibers [124,125]. Soy flour, containing 53% protein and up to 30% carbohydrate, is a cost-effective alternative to SPI and SPC [56,124]. However, poor interfacial adhesion between hydrophilic soy flour and nonpolar thermoplastic polymers leads to soy flour agglomeration, high melt viscosity, and interphase discontinuities. These discontinuities degrade the melt strength of soy flour(S)/linear low-density polyethylene (LLDPE) extrudate, preventing it from being drawn into fine fibers during melt spinning. Adding a compatibilizing monoglyceride (M) improves filler dispersion and reduces agglomerate sizes in the fiber [56]. Figure 1 showcases improved soy flour filler dispersion and reduced agglomerate sizes in the 23 wt.% S/7 wt.% M/70 wt.% LLDPE fiber compared to the 20 wt.% S/80 wt.% LLDPE fiber. Compatibilization enhances filler–matrix interactions, lowers melt viscosity, and improves extrudate melt strength. Due to the higher drawing of the fiber ensured by an increased melt strength, 23 wt.% S/7 wt.% M/70 wt.% LLDPE fiber demonstrates a smaller diameter ($45 \pm 11 \mu\text{m}$) compared to the 20 wt.% S/80 wt.% LLDPE fiber ($85 \pm 40 \mu\text{m}$). Additionally, fiber surface roughness due to soy flour agglomerates provides a more natural tactile feel to the soy flour/LLDPE fibers [56].

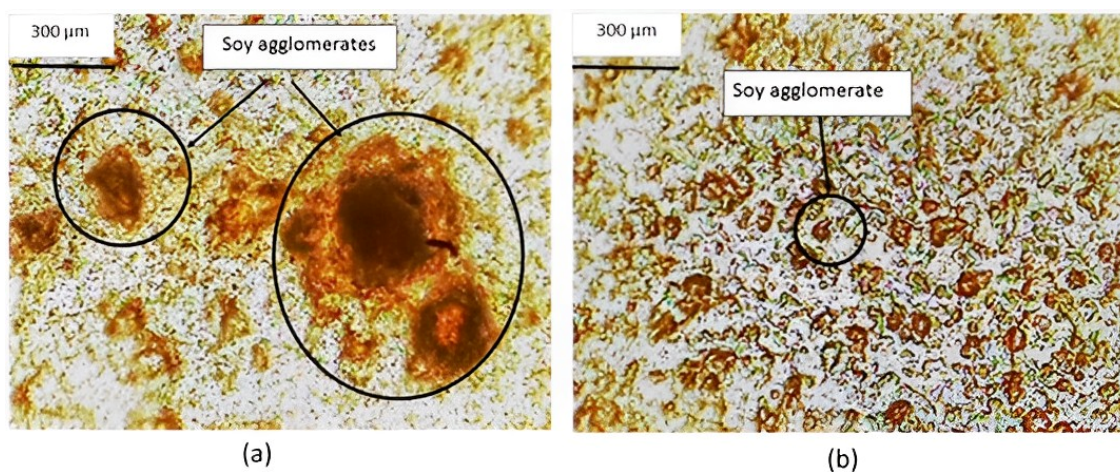


Figure 1. (a) Cross-sectional optical micrograph of soy flour/LLDPE blend (20 wt.% S, 80 wt.% LLDPE). (b) Optical micrograph of soy flour/monoglyceride/LLDPE blend (23 wt.% S, 7 wt.% M, 70 wt.% LLDPE). Reprinted from [56].

The fiber cross-section of the 30 wt.% S/20 wt.% M/50 wt.% LLDPE blend shows anisotropic filler volumetric dispersion. The monofilament interior holds a higher soy volumetric content than the surface. Increasing the LLDPE content in the blend at the expense of the compatibilizer and soy flour content, the protein–protein interactions appear to recede in favor of a more homogenous soy flour distribution between the monofilament interior and surface [25].

Soy flour exhibits degradation beyond $140\text{ }^{\circ}\text{C}$, making melt spinning with high-melting-point polymers like polypropylene (PP) challenging. At temperatures of $160\text{ }^{\circ}\text{C}$, $190\text{ }^{\circ}\text{C}$, $220\text{ }^{\circ}\text{C}$, and $250\text{ }^{\circ}\text{C}$ for 20 min, 30/70 wt.% monoglyceride compatibilized soy flour (SFM)/PP loses 0.5 wt.%, 1.8 wt.%, 5 wt.%, and 10 wt.% weight, respectively [55]. Spun 15/85 wt.% SFM/PP fibers display higher melt strength at $190\text{ }^{\circ}\text{C}$ and $200\text{ }^{\circ}\text{C}$, allowing fibers to draw finer diameters than at $160\text{ }^{\circ}\text{C}$ where the melt viscosity is high while strength is low. At $250\text{ }^{\circ}\text{C}$, soy flour degradation compromises melt strength, producing coarser fibers [55]. Yield stress behavior of 15/85 wt.% SFM/PP fiber resembles PP fiber at $160\text{ }^{\circ}\text{C}$ and $190\text{ }^{\circ}\text{C}$ but declines beyond these temperatures. Higher soy flour loading increases moisture absorption in the composite fiber, which is crucial for textile comfort. Polar groups on the fiber surface also aid in textile dyeing [55].

PLA composites with soy residue (30% protein product) and soy flour show a minimal 1% weight loss at slightly above $200\text{ }^{\circ}\text{C}$ and $230\text{ }^{\circ}\text{C}$ [126]. However, the composite's soy flour (SF) and soy residue (SR) contributions are not shared, nor is the exposure time to

these temperatures provided. PLA's higher thermal stability may account for the low mass loss observed. As observed in the case of SFM/PP fiber [55], increasing filler loading progressively diminishes the proclivity of the extruded fiber to draw to higher degrees [126]. At 5 wt.% filler loading, the SR/PLA spun fiber processed at a 230 °C temperature report SR/PLA exhibits higher modulus (1.6 ± 0.3 GPa) than SF/PLA (1.0 ± 0.4 GPa), which might be due to low protein thermal stability in high protein content-carrying SF. Both SR/PLA and SF/PLA fiber's tensile strength remains lower than PLA, attributed to polarity differences hindering the formation of a diffuse interface between the composite phases [126].

The biological components of soy protein/PE fiber make them susceptible to mold spoilage. Mold growth is observed in soy protein/PE fiber at all temperatures, with a water activity of 0.823 and beyond in all temperature regimes. Mold growth accelerates at water activity above 0.89 and temperatures exceeding 25 °C. Mold growth exhibits its slowest rate at a water activity of 0.87 and a temperature of 10 °C. A direct correlation exists between fiber's moisture absorption quantum and mold growth [125].

5.2.2. Wet Spinning

A suitable solvent dissolves the polymer in wet spinning to create a spinning solution. Next, the solution extrudes through a spinneret into a coagulation bath containing a nonsolvent. Solvent–nonsolvent exchange in the coagulation bath promotes extruded fiber precipitation. Finally, the fiber drawing takes place to achieve the required fiber linear density and enhance mechanical traits through molecular alignment.

Boyer et al.'s 1945 patent highlighted the importance of aged xanthate products in creating a stable, high-protein-content soy protein solution for wet spinning, preventing gelation. Despite a gradual decrease in viscosity over time, the solution remained wet-spinnable for up to 8 days, offering extended stability compared to alkaline solvents [15]. However, controlling protein solubility in the spinning solution was challenging due to soybean raw material variability [15,127]. The fibers achieved protein content ranging from 15 to 25 wt.% and had a linear density of 1.5 to 5 denier, according to the filed patent [15,127].

Huang et al. revived interest in soy protein fibers in general and RSPF in particular following earlier developments in the 1930s, 1940s, and 1950s [16]. Zein protein fiber wet spinning influenced their wet spinning method [54,128]. In Huang et al.'s work, sodium hydroxide managed the pH of the soy protein solution. They studied the impact of post-spinning treatment of wet-spun fibers with agents like acetic anhydride/acetic acid at 85 °C, acetaldehyde at room temperature, and glyoxal or glutaraldehyde at an acidic pH of 3.5 and room temperature. The soy protein solution viscosity increased with increasing soy protein content and pH value. Aqueous soy protein solutions with higher than 150 poise viscosity were challenging to spin through 386 µm holes of the spinneret. Wet-spun fibers coagulated in acid baths were weak, but salt addition improved strength, enabling post-treatment. They spun the best-performing wet-spun fiber with a soy protein content of 19.61 wt.%, a solution pH of 12.1, a coagulant consisting of 4% hydrochloric acid, 3.3% sodium chloride, 3.3% zinc chloride, and calcium chloride salts, post-treated it with 25% glutaraldehyde crosslinker, and finally drawn to 170% of its original length. Still, the best-performing wet-spun soy protein fiber was weaker than wool and acetate fibers at various water activity levels. Highly alkaline protein naturing at pH 12 can hydrolyze the protein backbone, negatively impacting the mechanical properties of the spun fiber [52].

The wet spinning of core–sheath soy protein/PVA fibers addresses the poor wet strength of monolithic soy protein fibers. Formaldehyde crosslinked soy protein/PVA fiber fractures the soy protein core but not the PVA sheath during drawing. Soy protein solution viscosity decreases due to polypeptide backbone degradation at pH 11.5 and when the alkali-denatured soy protein solution is heated to 45 °C, increasing core brittleness. In the case of denaturant addition, sodium sulfite has minimal impact on spinning solution viscosity, while urea causes a pronounced viscosity drop unrelated to protein degradation [73].

PVA aqueous solutions demonstrate improved spinnability at 70 °C, but high temperatures reduce viscosity in alkali-denatured protein solutions. To overcome this limitation, urea and sodium sulfite, combined with heat, effectively denature soy protein for wet spinning. The resulting denatured soy protein/PVA spinning solution possesses a suitable viscosity for the wet spinning of monolithic soy protein/PVA fibers. Increasing soy protein weight fraction in soy protein/PVA fibers decreases tensile modulus and elongation. Post-spinning glutaric dialdehyde crosslinking treatment enhances the mechanical properties of the soy protein/PVA fiber, improving modulus and breaking strength. After crosslinking, heat treatment under 20 MPa stress further enhances fiber performance. The soy protein/PVA hybrid fiber cross-section is circular compared to the neat PVA fiber's kidney-bean-shaped cross-section due to soy protein's slower coagulation rate [51].

Soy protein/alginate wet-spun fibers possess a high degree of compatibility between the two biopolymers. The coagulation bath for precipitating the soy protein/alginate solution contains calcium chloride, ethanol, and hydrochloric acid. Afterward, the formaldehyde solution crosslinks the coagulated fibers—coagulation bath with 50 wt.% ethanol content improves the soy protein/alginate fiber wet tensile strength and elongation at the break by 41.2% and 45.5%, respectively. Fiber with 10 wt.% soy protein content has optimal tensile characteristics with 14.1 cN/tex dry and 3.46 cN/tex wet strengths [50]. Hybrid fibers of casein protein (C) and soy protein (S), with diameters ranging from 100 to 250 μm , have been wet-spun. Pure casein fibers have a smooth surface and a circular shape. However, as the soy protein content increases in the hybrid fibers, surface roughness and irregularity become more prominent. Soy protein coagulates faster than casein, leading to non-circular shapes and hollowness in the fibers, as depicted in Figure 2. Notably, hybrid fibers exhibit superior thermal stability compared to pure soy or casein fibers, especially with higher soy protein content [129].

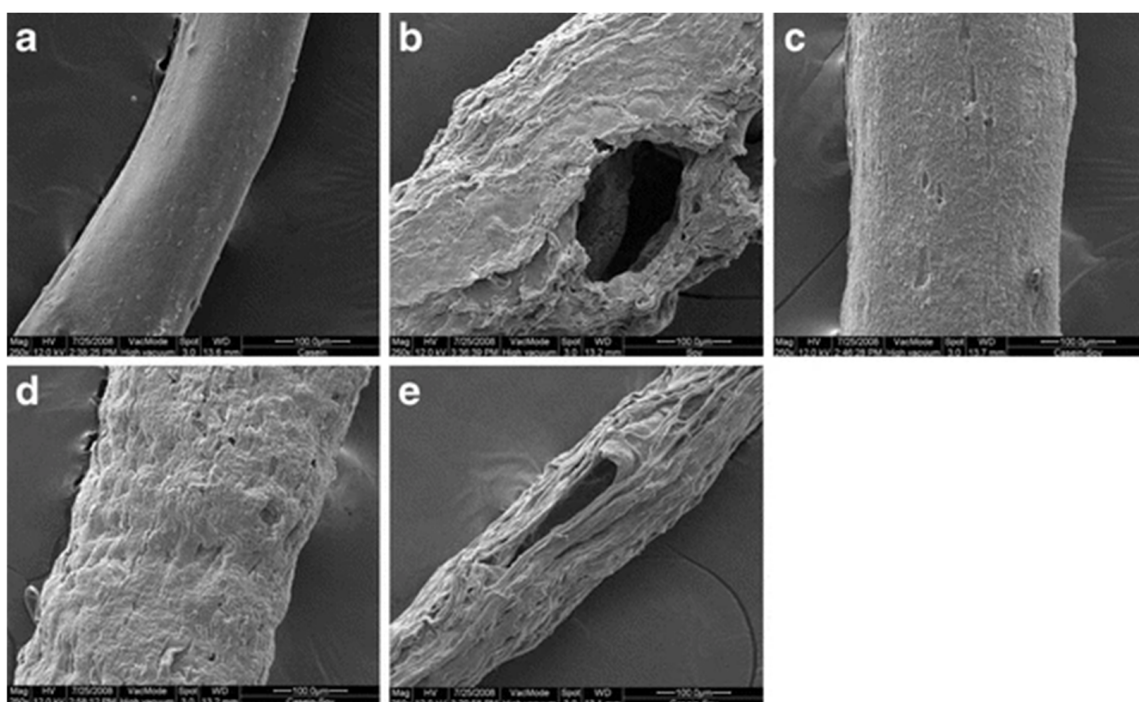


Figure 2. At a magnification of $\times 250$, the scanning electron micrographs display (a) casein fibers, (b) soy fibers, (c) hybrid fibers of C/S (75/25 wt.%), (d) hybrid fibers of C/S (50/50 wt.%), and (e) hybrid fibers of C/S (25/75 wt.%). Reprinted with permission from [129].

RSPF ranging from under 50 μm to 150 μm have been successfully wet-spun without post-treatment crosslinking [26,130]. Denaturation of soy protein occurs in a urea and sodium sulfite solution aged up to 96 h. The denatured soy protein spinning solution

solidifies in a sodium sulfite and acetic acid coagulation bath. Fibers spun from a spinning solution aged for 96 h exhibit a tensile strength of 145 MPa. In contrast, fibers spun from a 48 h-aged solution show a peak elongation at approximately 17%, after which it decreases. Aging protein solution for up to 48 h unfolds protein structure, increasing elongation, but after this, molecular crosslinking begins, decreasing elongation and increasing tensile strength. After 96 h, the protein's primary structure hydrolyzes, improving elongation but reducing tensile strength [26].

An optimum level of chain entanglements in polymeric solutions is crucial for wet spinnability. Among formic acid (95% concentration), pH 11 disodium hydrogen phosphate/sodium hydroxide alkali, and urea/reductant aqueous solutions, urea/reductant solution is the most effective in denaturing the protein without damaging the protein backbone. This solution also shows the highest chain entanglement compared to other acid and alkali solutions. Urea prevents aggregation of soy protein's hydrophobic regions, while the reductant prevents disulfide-bonded aggregates. Entanglement increases with soy protein concentration above 13% but slumps once it reaches 20% due to protein aggregation. Temperature indirectly affects entanglements in the spinning solutions. High-extrusion-rate shear enhances the spinnability of urea/reducing-agent-dissolved soy protein solutions by aligning the molecules in the flow direction. The soy protein spun fiber exhibits a strength of 1 g/denier, similar to wool fiber, with Young's modulus of 523 g/tex, greater than wool, while the strain at break is lower at 5 to 9% [52].

The wet spinning of hybrid hydrolyzed polyacrylonitrile (PAN) and soy protein hydrogel produces a fiber with increasing porosity as soy protein content rises, reducing the difference in porosities between shrunken and swollen conditions. Soy protein aggregation and hydrophobic bonding between hydrolyzed PAN molecules lead to partial phase separation in the hydrogel fiber. The degree of glutaraldehyde crosslinking in the hydrogel fiber shows a nonlinear correlation with equilibrium swelling elongation, but at higher soy protein contents, equilibrium swelling elongation slumps [130].

1-butyl-3-methylimidazolium chloride (BMIMCL) ionic liquid facilitates SPI denaturation at 70 °C by breaking covalent disulfide bonds and unfolding the protein. Denatured SPI is grafted with acrylonitrile to create SPI-g-PAN, which is then blended with pure PAN in DMSO/BMIMCL to form a 10 wt.% SPI wet spinning solution. Grafting and denaturation processes can decrease soy protein's molecular weight, which degrades vital rheological properties for fiber spinning like loss modulus, storage modulus, and complex viscosity. The resultant spun fiber has a porous cross-section [53], the reason for which has been explained [129]. Hot water fiber drawing at 95 °C lessens the porosity. In contrast, increasing draw ratios in hot water drawing has minimal impact on further porosity reduction due to fiber undergoing premature fracture before the pore collapse occurs. However, oven-drawn fibers at 110 °C achieve higher draw ratios and eliminate cross-sectional porosity. Figure 3 depicts the visible decline in cross-sectional porosity with increasing draw ratios using water bath and oven drawing. Porosity rationalization and molecular alignment due to higher fiber draw ratios boost the fiber elastic modulus and, interestingly, the strain at break, contrary to the typical regression with increasing draw ratios [53].

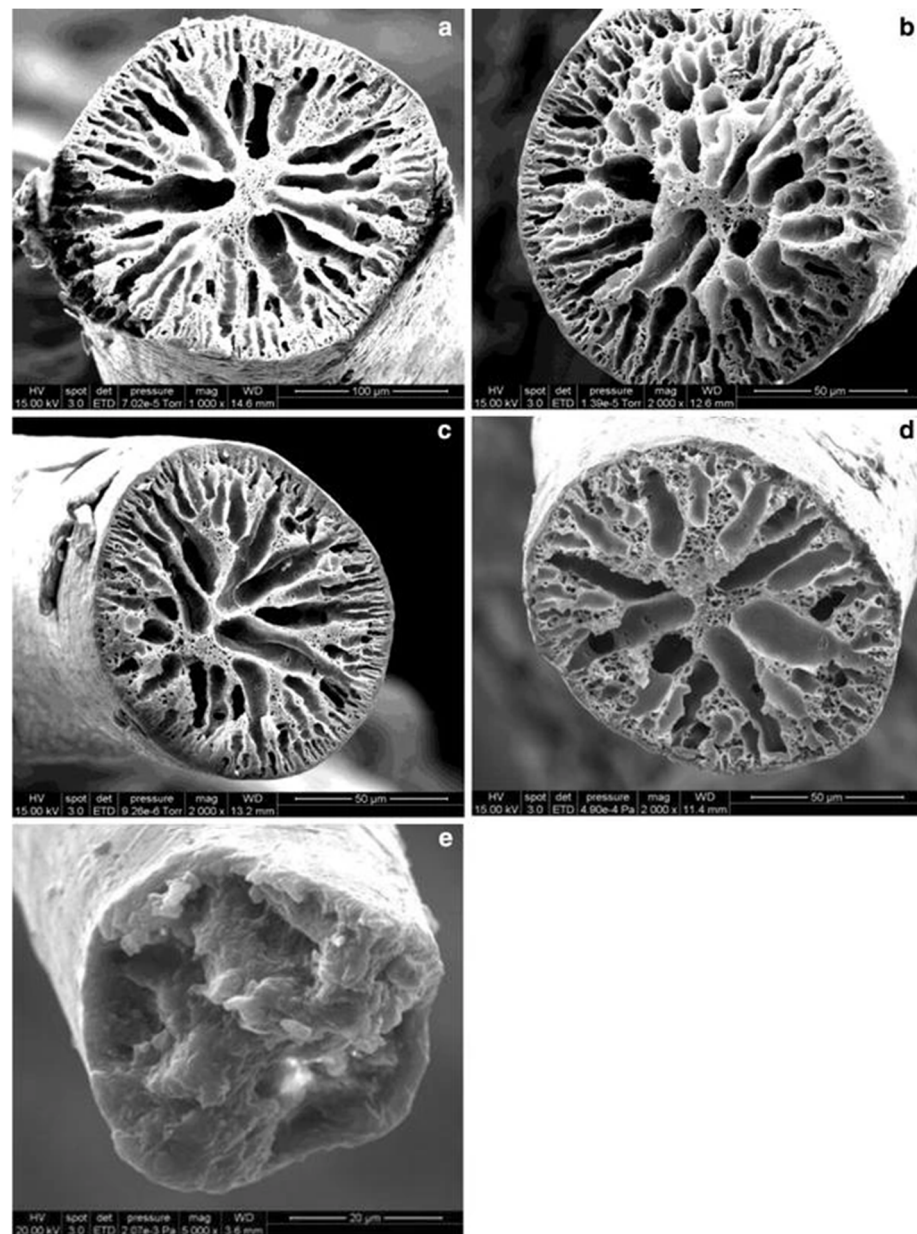


Figure 3. Investigating drawing effects on fiber morphology at ratios of (a) = 1, (b) = 2, (c) = 3, and (d) = 5 in hot water (95 °C for (a–d)) and an oven (110 °C for (e)). Analyzed cross-sections for insights. Reprinted with permission from [53].

6. Challenges and Opportunities

The objective of developing bio-based fibers is to provide a substitute for environmentally detrimental petroleum-based fibers. Regrettably, these environmentally harmful petroleum-based fibers fulfill the demand for high-volume textile applications. The success of a novel fiber in high-volume textile sectors like apparel, home textiles, and technical textiles hinges on its ability to satisfy the requisite performance standards for spinnability, weavability, and knittability. Soy protein fibers offer a promising avenue for utilizing low-value soy processing byproducts to benefit the agro and burgeoning green economies. Using soy protein byproducts in the textile industry provides exciting opportunities that remain ripe for exploration. However, to fully unlock the potential of this remarkable textile fiber, we must overcome certain limitations and explore specific opportunities.

6.1. Thermal Stability

Melt spinning is a scalable and eco-friendly technique that relies upon nonpolar thermoplastic polymers. The foremost roadblock to melt-spinning soy protein fiber is its thermal stability. Most thermoplastic polymer matrices melt at temperatures near or beyond the degradation temperature of soy protein. To achieve optimal melt viscosity, typically melt spinning involves conducting the process at temperatures 20 °C to 30 °C above the melting temperatures of thermoplastics; hence, coupled with prolonged thermal exposure at high temperatures during the melt spinning process, chances of protein degradation remain high.

6.2. Matrix Plasticization

A research gap exists in thermoplastic matrix plasticization to enable composite soy protein fibers to melt spin at lower temperatures. Plasticizing the matrix can eliminate the need for high processing temperatures and prolonged residence times in melt compounders at these temperatures to realize spinnable viscosities. This approach can prevent the decline of soy protein mechanical performance due to thermo-oxidative degradation.

6.3. Soy Protein Compatibility with Nonpolar Matrices and Functionalization Scope

Soy protein's limited compatibility with nonpolar thermoplastic matrices presents another formidable challenge. Denaturation under elevated temperatures exposes hydrophobic soy protein groups, which might improve their compatibility with the thermoplastic matrices. However, prolonged high-temperature exposure during melt spinning can lead to protein degradation and aggregation, compromising fiber mechanical properties and causing processing issues like spinneret hole plugging.

Soy protein possesses reactive amino, carboxyl, hydroxyl, sulfhydryl, and phosphate groups, rendering it a highly versatile biopolymer. The tunable nature of soy proteins amplifies their adaptability for various applications. Hence, the same tunability potential of soy protein structure can also facilitate weakening its hydrophilic character to improve its compatibility with nonpolar matrices.

6.4. Soy Protein Content

High soy protein content in the spun fibers is preferred to burnish their sustainability credentials. Furthermore, performance-wise, high soy protein content in soy fibers improves surface roughness, offering a desirable tactile feel and facilitating textile dyeability; however, wet-spun RSPF and melt-spun fibers with high soy protein content experience dominant protein–protein interactions, which lead to aggregation. These aggregates cause suboptimal extrudate viscosities, spinneret hole plugging, reduced soy protein solubility, and premature fiber failure during the mechanical performance-enhancing fiber drawing. Regulating and optimizing protein-to-protein interactions in the spinning melt or dope can be vital in managing spinning viscosities for obtaining high-quality fibers.

6.5. Mechanical Performance

Finally, and most importantly, the mechanical performance of developed soy protein fibers remains subpar when compared even to textile fibers at the lower end of the performance spectrum. Performance bottlenecks have prevented soy protein fibers from actualizing their potential to replace unsustainable textile fibers and thus require to be overcome.

Author Contributions: Conceptualization, M.T., A.L., A.-F.M.S., M.M., E.F. and T.T.; Methodology, M.T., A.L. and A.-F.M.S.; Validation, M.T., A.L., A.-F.M.S. and M.M.; Formal Analysis, M.T., A.L. and A.-F.M.S.; Investigation, M.T., A.L., A.-F.M.S., M.M., E.F. and T.T.; Resources, A.-F.M.S.; Data Curation, M.T., A.L. and E.F.; Writing—Original Draft Preparation, M.T.; Writing—Review and Editing, M.T., A.L., A.-F.M.S., M.M., E.F. and T.T.; Visualization, A.L. and M.T.; Supervision, A.-F.M.S., M.M., E.F. and T.T.; Project Administration, A.-F.M.S.; Funding Acquisition, A.-F.M.S. All authors have read and agreed to the published version of the manuscript.

Funding: This research received no specific grant from public, commercial, or not-for-profit funding agencies.

Conflicts of Interest: Thomas Theyson was employed by the TensTech Inc. The remaining authors declare that the research was conducted in the absence of any commercial or financial relationships that could be construed as a potential conflict of interest.

References

1. Geyer, R.; Jambeck, J.R.; Law, K.L. Production, use, and fate of all plastics ever made. *Sci. Adv.* **2017**, *3*, e1700782. [CrossRef]
2. Oliveri Conti, G.; Ferrante, M.; Banni, M.; Favara, C.; Nicolosi, I.; Cristaldi, A.; Fiore, M.; Zuccarello, P. Micro- and nano-plastics in edible fruit and vegetables. The first diet risks assessment for the general population. *Environ. Res.* **2020**, *187*, 109677. [CrossRef]
3. Pironti, C.; Ricciardi, M.; Motta, O.; Miele, Y.; Proto, A.; Montano, L. Microplastics in the Environment: Intake through the Food Web, Human Exposure and Toxicological Effects. *Toxics* **2021**, *9*, 224. [CrossRef]
4. Gasperi, J.; Wright, S.L.; Dris, R.; Collard, F.; Mandin, C.; Guerrouache, M.; Langlois, V.; Kelly, F.J.; Tassin, B. Microplastics in air: Are we breathing it in? *Curr. Opin. Environ. Sci. Health* **2018**, *1*, 1–5. [CrossRef]
5. Ragusa, A.; Svelato, A.; Santacroce, C.; Catalano, P.; Notarstefano, V.; Carnevali, O.; Papa, F.; Rongioletti, M.C.A.; Baiocco, F.; Draghi, S.; et al. Plasticenta: First evidence of microplastics in human placenta. *Environ. Int.* **2021**, *146*, 106274. [CrossRef]
6. Plastic Pollution Is Growing Relentlessly as Waste Management and Recycling Fall Short, Says OECD. Available online: <https://www.oecd.org/environment/plastic-pollution-is-growing-relentlessly-as-waste-management-and-recycling-fall-short.htm> (accessed on 2 June 2023).
7. Netravali, A.N.; Chabba, S. Composites get greener. *Mater. Today* **2003**, *6*, 22–29. [CrossRef]
8. Rahimizadeh, A.; Kalman, J.; Henri, R.; Fayazbakhsh, K.; Lessard, L. Recycled Glass Fiber Composites from Wind Turbine Waste for 3D Printing Feedstock: Effects of Fiber Content and Interface on Mechanical Performance. *Materials* **2019**, *12*, 3929. [CrossRef]
9. Boucher, J.; Friot, D. Primary Microplastics in the Oceans. IUCN. 2017. Available online: <https://portals.iucn.org/library/node/46622> (accessed on 2 June 2023).
10. Felgueiras, C.; Azoia, N.G.; Gonçalves, C.; Gama, M.; Dourado, F. Trends on the Cellulose-Based Textiles: Raw Materials and Technologies. *Front. Bioeng. Biotechnol.* **2021**, *9*, 608826. [CrossRef]
11. USDA ERS—Market Outlook. Available online: <https://www.ers.usda.gov/topics/crops/soybeans-and-oil-crops/market-outlook/> (accessed on 3 June 2023).
12. Association IS. Soybean Processing Growth Is Crushing It. Available online: <https://www.iasoybeans.com/newsroom/article/isr-january-2023-soybean-processing-growth-is-crushing-it> (accessed on 5 June 2023).
13. Soy Crush Rapidly Expands, Bringing Opportunity and Worries. DTN Progressive Farmer. 2023. Available online: <https://www.dtnpf.com/agriculture/web/ag/news/business-inputs/article/2022/05/13/soy-crush-rapidly-expands-bringing> (accessed on 5 June 2023).
14. Toshiji, K.; Ryohei, I. Process for Manufacturing Artificial Fiber from Protein Contained in Soybean. U.S. Patent US2198538A, 23 April 1940. Available online: <https://patents.google.com/patent/US2198538A/en> (accessed on 5 June 2023).
15. Boyer, R.A.; Atkinson, W.T.; Robinette, C.F. Artificial Fibers and Manufacture Thereof. U.S. Patent US2377854A, 12 June 1945. Available online: <https://patents.google.com/patent/US2377854A/en> (accessed on 5 June 2023).
16. Huang, H.C.; Hammond, E.G.; Reitmeier, C.A.; Myers, D.J. Properties of fibers produced from soy protein isolate by extrusion and wet-spinning. *J. Am. Oil Chem. Soc.* **1995**, *72*, 1453–1460. [CrossRef]
17. Kolbasov, A.; Sinha-Ray, S.; Joojode, A.; Hassan, M.A.; Brown, D.; Maze, B.; Pourdeyhimi, B.; Yarin, A.L. Industrial-Scale Solution Blowing of Soy Protein Nanofibers. *Ind. Eng. Chem. Res.* **2016**, *55*, 323–333. [CrossRef]
18. Ju, Z.; Lu, G.; Sheng, O.; Yuan, H.; Zhou, S.; Liu, T.; Liu, Y.; Wang, Y.; Nai, J.; Zhang, W.; et al. Soybean Protein Fiber Enabled Controllable Li Deposition and a LiF-Nanocrystal-Enriched Interface for Stable Li Metal Batteries. *Nano Lett.* **2022**, *22*, 1374–1381. [CrossRef]
19. Bhatia, J.K.; Kaith, B.S.; Singla, R.; Mehta, P.; Yadav, V.; Dhiman, J.; Bhatti, M.S. RSM optimized soy protein fibre as a sorbent material for treatment of water contaminated with petroleum products. *Desalination Water Treat.* **2016**, *57*, 4245–4254. [CrossRef]
20. Zhao, H.; Hou, L.; Lan, B.; Lu, Y. Fabrication of conductive soybean protein fiber for electromagnetic interference shielding through electroless copper plating. *J. Mater. Sci. Mater. Electron.* **2016**, *27*, 13300–13308. [CrossRef]
21. Wongkanya, R.; Chuysinuan, P.; Pengsuk, C.; Techasakul, S.; Lirdprapamongkol, K.; Svasti, J.; Nooeaid, P. Electrospinning of alginate/soy protein isolated nanofibers and their release characteristics for biomedical applications. *J. Sci. Adv. Mater. Devices* **2017**, *2*, 309–316. [CrossRef]
22. Gökgönül, G.B.; Sabir, E.C. An Experimental Study on Comparison of Selected Performance Properties of Soybean and Cotton Knitted Fabrics. *Çukurova Ünv. Mühendis. Fak. Derg.* **2022**, *37*, 803–812. [CrossRef]
23. Ferrándiz, M.; Fages, E.; Rojas-Lema, S.; Ivorra-Martinez, J.; Gomez-Caturla, J.; Torres-Giner, S. Development and Characterization of Weft-Knitted Fabrics of Naturally Occurring Polymer Fibers for Sustainable and Functional Textiles. *Polymers* **2021**, *13*, 665. [CrossRef]
24. Materials Market Report. Textile Exchange. 2023. Available online: <https://textileexchange.org/knowledge-center/reports/materials-market-report-2023/> (accessed on 7 February 2024).

25. Avinc, O.; Yavas, A.; Avinc, O.; Yavas, A. Soybean: For Textile Applications and Its Printing. In *Soybean—The Basis of Yield, Biomass and Productivity*; IntechOpen: London, UK, 2017. Available online: <https://www.intechopen.com/chapters/53674> (accessed on 7 February 2024).
26. Reddy, N.; Yang, Y. Soyprotein fibers with high strength and water stability for potential medical applications. *Biotechnol. Prog.* **2009**, *25*, 1796–1802. [CrossRef]
27. Brooks, M. Substitute Innovation: Rethinking the Failure of Mid-Twentieth Century Regenerated Protein Fibres and Their Legacy. Text Soc. Am. Symp. Proc. 1 September 2014. Available online: <https://digitalcommons.unl.edu/tsaconf/930> (accessed on 8 June 2023).
28. Aoyagi, W.S.A. *History of Soybeans and Soyfoods in Michigan (1853–2021): Extensively Annotated Bibliography and Sourcebook*; Soyinfo Center: Lafayette, CA, USA, 2021; 1217p.
29. Schmitz, J.F.; Erhan, S.Z.; Sharma, B.K.; Johnson, L.A.; Myers, D.J. 17—Biobased Products from Soybeans. In *Soybeans*; Johnson, L.A., White, P.J., Galloway, R., Eds.; AOCS Press: Champaign, IL, USA, 2008; pp. 539–612. Available online: <https://www.sciencedirect.com/science/article/pii/B9781893997646500202> (accessed on 10 June 2023).
30. Shurtleff, W.; Aoyagi, A. *Henry Ford and His Researchers—History of Their Work with Soybeans, Soyfoods and Chemurgy (1928–2011): Extensively Annotated Bibliography and Sourcebook*; Soyinfo Center: Lafayette, CA, USA, 2011; 437p.
31. Shurtleff, W.; Aoyagi, A. *History of Modern Soy Protein Ingredients—Isolates, Concentrates, and Textured Soy Protein Products (1911–2016)*; Soyinfo Center: Lafayette, CA, USA, 2016. Available online: <https://www.soyinfocenter.com/books/190> (accessed on 10 September 2023).
32. Shurtleff, W.; Aoyagi, A. *History of the Drackett Company's Work with Soybeans, Soy Protein and Azlon (1937–2020)—SoyInfo Center*; Soyinfo Center: Lafayette, CA, USA, 2020; 119p. Available online: <https://www.soyinfocenter.com/books/228> (accessed on 15 June 2023).
33. United States Office of War Information. *Information Digest*; Office of Government Reports; United States Office of War Information: Washington, DC, USA, 1942; 282p.
34. Seymour, R.B. Polymer Science before and after 1899: Notable Developments During the Lifetime of Maurits Dekker. *J. Macromol. Sci.—Chem.* **1989**, *26*, 1023–1032. [CrossRef]
35. Stenton, M.; Houghton, J.A.; Kapsali, V.; Blackburn, R.S. The Potential for Regenerated Protein Fibres within a Circular Economy: Lessons from the Past Can Inform Sustainable Innovation in the Textiles Industry. *Sustainability* **2021**, *13*, 2328. [CrossRef]
36. Berlan, J.P.; Bertrand, J.P.; Lebas, L. The growth of the American ‘soybean complex’. *Eur. Rev. Agric. Econ.* **1977**, *4*, 395–416. [CrossRef]
37. Improvements in or Relating to the Insolubilising Treatment of Films, Filaments, Fibres and Like Shaped Articles Made from Protein Solutions. GB605830A, 30 July 1948. Available online: <https://patents.google.com/patent/GB605830A/en?q=GB+605,830> (accessed on 13 June 2023).
38. Improvements in the Manufacture and Production of Artificial Filaments, Threads, Bands and the Like. GB614506A, 16 December 1948. Available online: <https://patents.google.com/patent/GB614506A/en?q=GB+605,830> (accessed on 14 June 2023).
39. Process for Improving the Properties of Protein Spinning Products. GB634812A, 29 March 1950. Available online: <https://patents.google.com/patent/GB634812A/en?q=GB+634,812> (accessed on 13 June 2023).
40. Wormell, R.L. *New Fibres from Proteins*; FAO: Rome, Italy, 1954.
41. Improvements in Regenerated Protein Fibres and Process for Preparation Thereof. GB638356A, 6 July 1950. Available online: <https://patents.google.com/patent/GB638356A/en?q=GB+638,356> (accessed on 13 June 2023).
42. Improvements in or Relating to a Method for Improving the Strength of Artificial Insolubilised Protein Filaments or Fibres. GB665462A, 1952. Available online: <https://patents.google.com/patent/GB665462A/en?q=GB+665,462> (accessed on 13 June 2023).
43. Improvements in and Relating to the Production of Artificial Protein Fibres. GB674755A, 7 February 1952. Available online: <https://patents.google.com/patent/GB674755A/en?q=GB+674,755> (accessed on 14 June 2023).
44. Louis, W.R. Production of Artificial Filaments, Threads, Fibres, Bands, and the Like. U.S. Patent US2775506A, 25 December 1956. Available online: <https://patents.google.com/patent/US2775506A/en?q=GB+605,830> (accessed on 14 June 2023).
45. Method and Apparatus for Forming Fibers. GB862428A, 8 March 1961. Available online: <https://patents.google.com/patent/GB862428A/en?q=GB+862,428> (accessed on 14 June 2023).
46. Colton, J.B.; Burns, B.R.; Knapp, F.D. Plastic particles in surface waters of the northwestern atlantic. *Science* **1974**, *185*, 491–497. [CrossRef]
47. Brooks, M.M. 7—Regenerated protein fibres: A preliminary review. In *Handbook of Textile Fibre Structure*; Eichhorn, S.J., Hearle, J.W.S., Jaffe, M., Kikutani, T., Eds.; Woodhead Publishing Series in Textiles; Woodhead Publishing: Shaston, UK, 2009; Volume 2, pp. 234–265. Available online: <https://www.sciencedirect.com/science/article/pii/B978184569730350007X> (accessed on 16 June 2023).
48. Wang, Y. New Materials in Textile Innovation. *J. Mater. Process. Des.* **2023**, *7*, 32–40.
49. Jackman, D.R.; Dixon, M.K.; Condra, J. *The Guide to Textiles for Interiors*; Portage & Main Press: Winnipeg, MB, Canada, 2003; 248p.
50. Wang, Q.; Du, Y.; Hu, X.; Yang, J.; Fan, L.; Feng, T. Preparation of alginate/soy protein isolate blend fibers through a novel coagulating bath. *J. Appl. Polym. Sci.* **2006**, *101*, 425–431. [CrossRef]

51. Zhang, X.; Min, B.G.; Kumar, S. Solution spinning and characterization of poly(vinyl alcohol)/soybean protein blend fibers. *J. Appl. Polym. Sci.* **2003**, *90*, 716–721. [[CrossRef](#)]
52. Mu, B.; Xu, H.; Li, W.; Xu, L.; Yang, Y. Spinnability and rheological properties of globular soy protein solution. *Food Hydrocoll.* **2019**, *90*, 443–451. [[CrossRef](#)]
53. Deng, S.; Cheng, J.; Guo, X.; Jiang, L.; Zhang, J. Fiber Spinning of Polyacrylonitrile Grafted Soy Protein in an Ionic Liquid/DMSO Mixture Solvent. *J. Polym. Environ.* **2014**, *22*, 17–26. [[CrossRef](#)]
54. Zhang, M.; Reitmeier, C.A.; Hammond, E.G.; Myers, D.J. Production of Textile Fibers from Zein and a Soy Protein-Zein Blend. *Cereal Chem.* **1997**, *74*, 594–598. [[CrossRef](#)]
55. Guzdemir, O.; Ogale, A.A. Influence of Spinning Temperature and Filler Content on the Properties of Melt-Spun Soy Flour/Polypropylene Fibers. *Fibers* **2019**, *7*, 83. [[CrossRef](#)]
56. Guzdemir, O.; Lukubira, S.; Ogale, A.A. Soy-filled polyethylene fibers for modified surface and hydrophilic characteristics. *J. Appl. Polym. Sci.* **2018**, *135*, 46609. [[CrossRef](#)]
57. Wong, D.W.S. (Ed.) Proteins. In *Mechanism and Theory in Food Chemistry*, 2nd ed.; Springer International Publishing: Cham, Switzerland, 2018; pp. 55–122. [[CrossRef](#)]
58. Alberts, B.; Johnson, A.; Lewis, J.; Raff, M.; Roberts, K.; Walter, P. The Shape and Structure of Proteins. In *Molecular Biology of the Cell*, 4th ed.; Garland Science: New York, NY, USA, 2002. Available online: <https://www.ncbi.nlm.nih.gov/books/NBK26830/> (accessed on 2 July 2023).
59. Kinsella, J.E. Functional properties of soy proteins. *J. Am. Oil Chem. Soc.* **1979**, *56 Pt 1*, 242–258. [[CrossRef](#)]
60. Sui, X.; Zhang, T.; Jiang, L. Soy Protein: Molecular Structure Revisited and Recent Advances in Processing Technologies. *Annu. Rev. Food Sci. Technol.* **2021**, *12*, 119–147. [[CrossRef](#)] [[PubMed](#)]
61. Witte, N.H. Chapter 7—Soybean Meal Processing and Utilization. In *Practical Handbook of Soybean Processing and Utilization*; Erickson, D.R., Ed.; AOCS Press: Champaign, IL, USA, 1995; pp. 93–116. Available online: <https://www.sciencedirect.com/science/article/pii/B9780935315639500115> (accessed on 18 June 2023).
62. Ly, Y.T.P.; Johnson, L.A.; Jane, J. Soy Protein As Biopolymer. In *Biopolymers from Renewable Resources*; Kaplan, D.L., Ed.; Macromolecular Systems—Materials Approach; Springer: Berlin/Heidelberg, Germany, 1998; pp. 144–176. [[CrossRef](#)]
63. Lusas, E.W.; Rhee, K.C. Chapter 8—Soy Protein Processing and Utilization. In *Practical Handbook of Soybean Processing and Utilization*; Erickson, D.R., Ed.; AOCS Press: Champaign, IL, USA, 1995; pp. 117–160. Available online: <https://www.sciencedirect.com/science/article/pii/B9780935315639500127> (accessed on 20 June 2023).
64. Mäkinen, O.E.; Zannini, E.; Koehler, P.; Arendt, E.K. Heat-denaturation and aggregation of quinoa (*Chenopodium quinoa*) globulins as affected by the pH value. *Food Chem.* **2016**, *196*, 17–24. [[CrossRef](#)] [[PubMed](#)]
65. Jiang, J.; Shi, L.; Ren, Z.; Weng, W. Preparation and characterization of soy protein isolate films by pretreatment with cysteine. *Food Chem. X* **2023**, *18*, 100735. [[CrossRef](#)] [[PubMed](#)]
66. Asakura, T.; Adachi, K.; Schwartz, E. Stabilizing effect of various organic solvents on protein. *J. Biol. Chem.* **1978**, *253*, 6423–6425. [[CrossRef](#)] [[PubMed](#)]
67. Sinha, R.; Khare, S.K. Protective role of salt in catalysis and maintaining structure of halophilic proteins against denaturation. *Front. Microbiol.* **2014**, *5*, 80043. [[CrossRef](#)] [[PubMed](#)]
68. Joyce, A.M.; Kelly, A.L.; O'Mahony, J.A. Controlling denaturation and aggregation of whey proteins during thermal processing by modifying temperature and calcium concentration. *Int. J. Dairy Technol.* **2018**, *71*, 446–453. [[CrossRef](#)]
69. Schön, A.; Clarkson, B.R.; Siles, R.; Ross, P.; Brown, R.K.; Freire, E. Denatured state aggregation parameters derived from concentration dependence of protein stability. *Anal. Biochem.* **2015**, *488*, 45–50. [[CrossRef](#)]
70. Zheng, Z.; Xin, C.; Li, Y. Numerical study on mechanisms of soy protein as a functional modifier for polymer materials. *Model. Simul. Mater. Sci. Eng.* **2019**, *27*, 085010. [[CrossRef](#)]
71. Yue, L.; Meng, Z.; Yi, Z.; Gao, Q.; Mao, A.; Li, J. Effects of Different Denaturants on Properties and Performance of Soy Protein-Based Adhesive. *Polymers* **2019**, *11*, 1262. [[CrossRef](#)] [[PubMed](#)]
72. O'Flynn, T.D.; Hogan, S.A.; Daly, D.F.M.; O'Mahony, J.A.; McCarthy, N.A. Rheological and Solubility Properties of Soy Protein Isolate. *Molecules* **2021**, *26*, 3015. [[CrossRef](#)]
73. Zhang, Y.; Ghasemzadeh, S.; Kotliar, A.M.; Kumar, S.; Presnell, S.; Williams, L.D. Fibers from soybean protein and poly(vinyl alcohol). *J. Appl. Polym. Sci.* **1999**, *71*, 11–19. [[CrossRef](#)]
74. Renkema, J.M.S.; Gruppen, H.; van Vliet, T. Influence of pH and ionic strength on heat-induced formation and rheological properties of soy protein gels in relation to denaturation and their protein compositions. *J. Agric. Food Chem.* **2002**, *50*, 6064–6071. [[CrossRef](#)] [[PubMed](#)]
75. El-Adawy, T.A. Functional properties and nutritional quality of acetylated and succinylated mung bean protein isolate. *Food Chem.* **2000**, *70*, 83–91. [[CrossRef](#)]
76. Barman, B.G.; Hansen, J.R.; Mossey, A.R. Modification of the physical properties of soy protein isolate by acetylation. *J. Agric. Food Chem.* **1977**, *25*, 638–641. [[CrossRef](#)] [[PubMed](#)]
77. Kim, K.S.; Rhee, J.S. Effects of Acetylation on Physicochemical Properties of J1s Soy Protein. *J. Food Biochem.* **1989**, *13*, 187–199. [[CrossRef](#)]
78. Allen, K.A. Study of Mechanical and Thermal Properties of Soy Flour Elastomers. Ph.D. Thesis, Iowa State University, Ames, IA, USA, 2014. Available online: <https://ui.adsabs.harvard.edu/abs/2014PhDT.....173A> (accessed on 26 July 2023).

79. Foulk, J.A.; Bunn, J.M. Properties of compression-molded, acetylated soy protein films. *Ind. Crops Prod.* **2001**, *14*, 11–22. [CrossRef]
80. Sitohy, M.; Osman, A. Antimicrobial activity of native and esterified legume proteins against Gram-negative and Gram-positive bacteria. *Food Chem.* **2010**, *120*, 66–73. [CrossRef]
81. Wang, T.; Yi, K.; Li, Y.; Wang, H.; Fan, Z.; Jin, H.; Xu, J. Esterified Soy Proteins with Enhanced Antibacterial Properties for the Stabilization of Nano-Emulsions under Acidic Conditions. *Molecules* **2023**, *28*, 3078. [CrossRef] [PubMed]
82. Pattanaik, S.; Sutar, A.K.; Maharana, T. Graft copolymerization of Soy Protein Isolate with Polylactide via Ring Opening Polymerization. *IOP Conf. Ser. Mater. Sci. Eng.* **2018**, *410*, 012011. [CrossRef]
83. Feng, B.; Wang, D.; Li, Y.; Qian, J.; Yu, C.; Wang, M.; Luo, D.; Wei, S. Mechanical Properties of a Soy Protein Isolate–Grafted–Acrylate (SGA) Copolymer Used for Wood Coatings. *Polymers* **2020**, *12*, 1137. [CrossRef] [PubMed]
84. Zhang, Z.; Jiang, G.; Pang, J.; Su, L. Synthesis of renewable soybean protein and acrylate copolymers via ATRP in ionic liquid. *Ind. Crops Prod.* **2022**, *180*, 114720. [CrossRef]
85. Zhao, Y.; Xu, H.; Mu, B.; Xu, L.; Yang, Y. Biodegradable soy protein films with controllable water solubility and enhanced mechanical properties via graft polymerization. *Polym. Degrad. Stab.* **2016**, *133*, 75–84. [CrossRef]
86. Bhardwaj, P.; Kalia, S.; Kumar, A.; Mittal, H. Peroxide Treatment of Soy Protein Fibers Followed by Grafting of Poly(methyl acrylate) and Copolymers. *J. Renew. Mater.* **2013**, *1*, 302–310. [CrossRef]
87. Doshi, J.; Reneker, D.H. Electrospinning process and applications of electrospun fibers. *J. Electrostat.* **1995**, *35*, 151–160. [CrossRef]
88. Anton, F. Process and Apparatus for Preparing Artificial Threads. U.S. Patent US1975504A, 2 October 1934. Available online: <https://patents.google.com/patent/US1975504A/en> (accessed on 5 February 2024).
89. Liu, H.; Slamovich, E.B.; Webster, T.J. Less harmful acidic degradation of poly(lactico-glycolic acid) bone tissue engineering scaffolds through titania nanoparticle addition. *Int. J. Nanomed.* **2006**, *1*, 541–545. [CrossRef] [PubMed]
90. Chacko, B.K.; Chandler, R.T.; Mundhekar, A.; Khoo, N.; Pruitt, H.M.; Kucik, D.F.; Parks, D.A.; Kevil, C.G.; Barnes, S.; Patel, R.P. Revealing anti-inflammatory mechanisms of soy isoflavones by flow: Modulation of leukocyte-endothelial cell interactions. *Am. J. Physiol. Heart Circ. Physiol.* **2005**, *289*, H908–H915. [CrossRef] [PubMed]
91. Har-el, Y.E.; Gerstenhaber, J.A.; Brodsky, R.; Huneke, R.B.; Lelkes, P.I. Electrospun soy protein scaffolds as wound dressings: Enhanced reepithelialization in a porcine model of wound healing. *Wound Med.* **2014**, *5*, 9–15. [CrossRef]
92. Visakh, P.M.; Nazarenko, O.B. *Soy Protein-Based Blends, Composites and Nanocomposites*; John Wiley & Sons: Hoboken, NJ, USA, 2017; 275p.
93. Santin, M.; Ambrosio, L. Soybean-based biomaterials: Preparation, properties and tissue regeneration potential. *Expert Rev. Med. Devices* **2008**, *5*, 349–358. [CrossRef] [PubMed]
94. Tokudome, Y.; Nakamura, K.; Kage, M.; Todo, H.; Sugibayashi, K.; Hashimoto, F. Effects of soybean peptide and collagen peptide on collagen synthesis in normal human dermal fibroblasts. *Int. J. Food Sci. Nutr.* **2012**, *63*, 689–695. [CrossRef] [PubMed]
95. Khabbaz, B.; Solouk, A.; Mirzadeh, H. Polyvinyl alcohol/soy protein isolate nanofibrous patch for wound-healing applications. *Prog. Biomater.* **2019**, *8*, 185–196. [CrossRef] [PubMed]
96. Phelan, M.A.; Kruczek, K.; Wilson, J.H.; Brooks, M.J.; Drinnan, C.T.; Regent, F.; Gerstenhaber, J.A.; Swaroop, A.; Lelkes, P.I.; Li, T. Soy Protein Nanofiber Scaffolds for Uniform Maturation of Human Induced Pluripotent Stem Cell-Derived Retinal Pigment Epithelium. *Tissue Eng. Part C Methods* **2020**, *26*, 433–446. [CrossRef] [PubMed]
97. Ahmadian, S.; Ghorbani, M.; Mahmoodzadeh, F. Silver sulfadiazine-loaded electrospun ethyl cellulose/polylactic acid/collagen nanofibrous mats with antibacterial properties for wound healing. *Int. J. Biol. Macromol.* **2020**, *162*, 1555–1565. [CrossRef] [PubMed]
98. Popov Pereira da Cunha, M.D.; Aldana, A.A.; Abraham, G.A. Photo-crosslinked soy protein-based electrospun scaffolds. *Mater. Lett. X* **2021**, *12*, 100115. [CrossRef]
99. Popov Pereira da Cunha, M.D.; Ponce, A.G.; Abraham, G.A. Effect of thermal treatments and UV radiation on green soy protein isolated crosslinked electrospun mats. *J. Appl. Polym. Sci.* **2023**, *140*, e53777. [CrossRef]
100. Lin, L. Electrospun Soy Protein-based Scaffolds for Skin Tissue Engineering and Wound Healing. Ph.D. Thesis, Drexel University, Philadelphia, PA, USA, 2011.
101. Ramji, K.; Shah, R.N. Electrospun soy protein nanofiber scaffolds for tissue regeneration. *J. Biomater. Appl.* **2014**, *29*, 411–422. [CrossRef] [PubMed]
102. Cai, N.; Dai, Q.; Wang, Z.; Luo, X.; Xue, Y.; Yu, F. Toughening of electrospun poly(l-lactic acid) nanofiber scaffolds with unidirectionally aligned halloysite nanotubes. *J. Mater. Sci.* **2015**, *50*, 1435–1445. [CrossRef]
103. Cho, D.; Nnadi, O.; Netravali, A.; Joo, Y.L. Electrospun Hybrid Soy Protein/PVA Fibers. *Macromol. Mater. Eng.* **2010**, *295*, 763–773. [CrossRef]
104. Delyanee, M.; Solouk, A.; Akbari, S.; Daliri Joupari, M. Engineered hemostatic bionanocomposite of poly(lactic acid) electrospun mat and amino-modified halloysite for potential application in wound healing. *Polym. Adv. Technol.* **2021**, *32*, 3934–3947. [CrossRef]
105. Doustdar, F.; Ramezani, S.; Ghorbani, M.; Mortazavi Moghadam, F. Optimization and characterization of a novel tea tree oil-integrated poly(ϵ -caprolactone)/soy protein isolate electrospun mat as a wound care system. *Int. J. Pharm.* **2022**, *627*, 122218. [CrossRef]
106. Xu, X.; Jiang, L.; Zhou, Z.; Wu, X.; Wang, Y. Preparation and Properties of Electrospun Soy Protein Isolate/Polyethylene Oxide Nanofiber Membranes. *ACS Appl. Mater. Interfaces* **2012**, *4*, 4331–4337. [CrossRef] [PubMed]

107. Varshney, N.; Sahi, A.K.; Poddar, S.; Mahto, S.K. Soy protein isolate supplemented silk fibroin nanofibers for skin tissue regeneration: Fabrication and characterization. *Int. J. Biol. Macromol.* **2020**, *160*, 112–127. [[CrossRef](#)] [[PubMed](#)]
108. Doustdar, F.; Ghorbani, M. ZIF-8 enriched electrospun ethyl cellulose/polyvinylpyrrolidone scaffolds: The key role of polyvinylpyrrolidone molecular weight. *Carbohydr. Polym.* **2022**, *291*, 119620. [[CrossRef](#)] [[PubMed](#)]
109. Sampath Kumar, N.; Santhosh, C.; Vathaluru Sudakaran, S.; Deb, A.; Raghavan, V.; Venugopal, V.; Bhatnagar, A.; Bhat, S.; Andrews, N.G. Electrospun polyurethane and soy protein nanofibres for wound dressing applications. *IET Nanobiotechnol.* **2017**, *12*, 94–98. [[CrossRef](#)]
110. Amjadi, S.; Almasi, H.; Ghorbani, M.; Ramazani, S. Preparation and characterization of TiO₂NPs and betanin loaded zein/sodium alginate nanofibers. *Food Packag. Shelf Life* **2020**, *24*, 100504. [[CrossRef](#)]
111. Tansaz, S.; Liverani, L.; Vester, L.; Boccaccini, A.R. Soy protein meets bioactive glass: Electrospun composite fibers for tissue engineering applications. *Mater. Lett.* **2017**, *199*, 143–146. [[CrossRef](#)]
112. Jaberifard, F.; Ramezani, S.; Ghorbani, M.; Arsalani, N.; Mortazavi Moghadam, F. Investigation of wound healing efficiency of multifunctional eudragit/soy protein isolate electrospun nanofiber incorporated with ZnO loaded halloysite nanotubes and allantoin. *Int. J. Pharm.* **2023**, *630*, 122434. [[CrossRef](#)] [[PubMed](#)]
113. White, C.; DiStefano, T.; Olabisi, R. The influence of substrate modulus on retinal pigment epithelial cells. *J. Biomed. Mater. Res. A* **2017**, *105*, 1260–1266. [[CrossRef](#)] [[PubMed](#)]
114. Wang, S.; Marcone, M.F.; Barbut, S.; Lim, L.T. Electrospun soy protein isolate-based fiber fortified with anthocyanin-rich red raspberry (*Rubus strigosus*) extracts. *Food Res. Int.* **2013**, *52*, 467–472. [[CrossRef](#)]
115. Vega-Lugo, A.C.; Lim, L.T. Electrospinning of Soy Protein Isolate Nanofibers. *J. Biobased Mater. Bioenergy* **2008**, *2*, 223–230. [[CrossRef](#)]
116. Vega-Lugo, A.C.; Lim, L.T. Controlled release of allyl isothiocyanate using soy protein and poly(lactic acid) electrospun fibers. *Food Res. Int.* **2009**, *42*, 933–940. [[CrossRef](#)]
117. Daristotle, J.L.; Behrens, A.M.; Sandler, A.D.; Kofinas, P. A Review of the Fundamental Principles and Applications of Solution Blow Spinning. *ACS Appl. Mater. Interfaces* **2016**, *8*, 34951–34963. [[CrossRef](#)] [[PubMed](#)]
118. Kolbasov, A.; Sinha-Ray, S.; Yarin, A.L.; Pourdeyhimi, B. Heavy metal adsorption on solution-blown biopolymer nanofiber membranes. *J. Membr. Sci.* **2017**, *530*, 250–263. [[CrossRef](#)]
119. Zhang, Y.; Lee, M.W.; An, S.; Sinha-Ray, S.; Khansari, S.; Joshi, B.; Hong, S.; Hong, J.H.; Kim, J.J.; Pourdeyhimi, B.; et al. Antibacterial activity of photocatalytic electrospun titania nanofiber mats and solution-blown soy protein nanofiber mats decorated with silver nanoparticles. *Catal. Commun.* **2013**, *34*, 35–40. [[CrossRef](#)]
120. Penconek, A.; Kasak, D.; Moskal, A. Soy Protein Nanofibers Obtained by Solution Blow Spinning. *Processes* **2023**, *11*, 2310. [[CrossRef](#)]
121. Sinha-Ray, S.; Khansari, S.; Yarin, A.L.; Pourdeyhimi, B. Effect of Chemical and Physical Cross-Linking on Tensile Characteristics of Solution-Blown Soy Protein Nanofiber Mats. *Ind. Eng. Chem. Res.* **2012**, *51*, 15109–15121. [[CrossRef](#)]
122. Sinha-Ray, S.; Zhang, Y.; Yarin, A.L.; Davis, S.C.; Pourdeyhimi, B. Solution Blowing of Soy Protein Fibers. *Biomacromolecules* **2011**, *12*, 2357–2363. [[CrossRef](#)] [[PubMed](#)]
123. Khansari, S.; Sinha-Ray, S.; Yarin, A.L.; Pourdeyhimi, B. Stress-strain dependence for soy-protein nanofiber mats. *J. Appl. Phys.* **2012**, *111*, 044906. [[CrossRef](#)]
124. Guzdemir, O. Melt-Spinning and Properties of Soy-Filled Polyethylene, Polypropylene, and Poly-(Lactic Acid) Fibers. Diss. 1 August 2019. Available online: https://tigerprints.clemson.edu/all_dissertations/2439 (accessed on 19 July 2023).
125. Naphade, C.; Han, I.; Lukubira, S.; Ogale, A.; Rieck, J.; Dawson, P. Prediction of Mold Spoilage for Soy/Polyethylene Composite Fibers. *Int. J. Polym. Sci.* **2015**, *2015*, e176826. [[CrossRef](#)]
126. Güzdemir, Ö.; Bermudez, V.; Kanhere, S.; Ogale, A.A. Melt-spun poly(lactic acid) fibers modified with soy fillers: Toward environment-friendly disposable nonwovens. *Polym. Eng. Sci.* **2020**, *60*, 1158–1168. [[CrossRef](#)]
127. Boyer, R.A. Soybean Protein Fibers Experimental Production. *Ind. Eng. Chem.* **1940**, *32*, 1549–1551. [[CrossRef](#)]
128. Croston, C.B.; Evans, C.D.; Smith, A.K. Zein Fibers. *Ind. Eng. Chem.* **1945**, *37*, 1194–1198. [[CrossRef](#)]
129. Sudha, T.B.; Thanikaivelan, P.; Ashokkumar, M.; Chandrasekaran, B. Structural and thermal investigations of biomimetically grown casein-soy hybrid protein fibers. *Appl. Biochem. Biotechnol.* **2011**, *163*, 247–257. [[CrossRef](#)] [[PubMed](#)]
130. Yu, L.; Gu, L. Hydrolyzed polyacrylonitrile-blend-soy protein hydrogel fibers: A study of structure and dynamic pH response. *Polym. Int.* **2009**, *58*, 66–73. [[CrossRef](#)]

Disclaimer/Publisher's Note: The statements, opinions and data contained in all publications are solely those of the individual author(s) and contributor(s) and not of MDPI and/or the editor(s). MDPI and/or the editor(s) disclaim responsibility for any injury to people or property resulting from any ideas, methods, instructions or products referred to in the content.